Characterization of a High-Energy X-ray Compound Refractive Lens

Stewart Laird
Advisor: Dr. Jim Knauer

Traditionally, high energy x rays are notoriously hard to focus for imaging purposes due to an extremely low degree of refraction in solids. Using a device composed of many small adjacent lenses (a Compound Refractive Lens, or "CRL") it is possible to achieve images with much better resolution than current methods of high-energy x-ray imaging such as pinhole cameras. The literature shows potential resolutions of 1-2 μm for a CRL x-ray lens. An image resolution of smaller than 5 microns would allow accurate imaging of the 20-50 micron core of fusion implosions in the Omega laser system. A commercial compound refractive lens has been purchased and analyzed experimentally for image resolution and quality. Preliminary data has suggested that with proper alignment and focus, resolutions of 6.8 +/- 1.5 microns or better are possible. As long as no significant spherical or chromatic aberrations appear, this data would encourage future research into implementing CRL technology into existing Omega camera mounts.

The motivation for integrating compound refractive lenses (CRLs) into the LLE Omega system lies in the fact that CRLs can provide high resolution images of high energy x rays. During fusion implosions, there are three types of radiation emitted that are useful for imaging: neutrons, gamma rays, and X rays. Neutrons are emitted primarily in areas with high density and high temperature and therefore are a prime candidate for imaging regions where fusion is occurring. However, the highest resolution that has been achieved thus far with neutron imaging is greater than 50 microns. Gamma rays are emitted from the matter evaporated
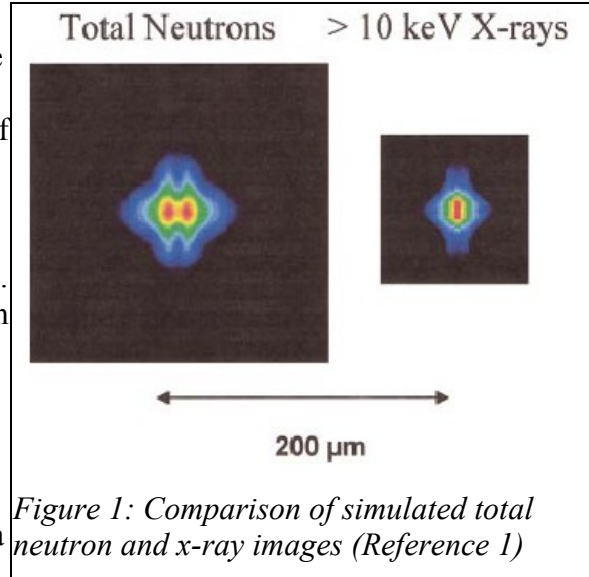

Figure 1: Comparison of simulated total neutron and x-ray images (Reference 1)

off the target, and therefore do not provide a useful image of the fusion core. High energy x rays, as shown in a simulation done at Los Alamos (Figure 1), are emitted from the same high interest areas of the implosion. High energy x rays are difficult to image due to high absorption and low refraction in solids. However, CRLs are capable of overcoming these obstacles and achieving very high resolutions. Although CRLs are designed to circumvent the difficulties of high-energy x-ray propagation, they introduce some other problems such as precision alignment and are not able to compensate for chromatic aberration, a factor that results in a large reduction in image quality when using a polychromatic source.

The low refraction and chromatic aberration result from high-energy X ray's abnormal behavior in solids. The complex index of refraction is given by the equation

$$n = 1 - \delta - i\beta$$

where n is the index of refraction, δ is the real refractive index decrement, and β is the imaginary absorption factor. The complex index of refraction can also be expressed by the equation

$$n = 1 - \frac{r_0}{2\pi} \lambda^2 \sum_q n_q f_q(0)$$

where n is the index of refraction, r_0 is the classical electron radius, λ is the wavelength of the interacting x ray, n_q is the number of atoms q per unit volume, and f_q is the atomic scattering factor of that atom, a complex number determined for each atom.

For most solids the refractive index n increases with n_q. However, for x rays n decreases as n_q increases. This is due to the fact that the high frequency of x rays causes them to interact with most solids as plasmas, interacting with the outer electrons. The consequence of this is that for a converging lens, a concave lens shape is necessary. δ is also very small for high energy x rays, generally between 10^{-5} and 10^{-7}. The consequence

of this is that x rays have only a very small degree of refraction through a single lens. Also, these equations show that δ and λ^2 are directly proportional, which will become relevant when looking at the effects of large wavelength bandwidth sources on the focal length. The equation (Reference 2)

$$f = \frac{r}{2N\delta}$$

where f is the focal length, r is the radius of a lens, N is the number of lenses and δ is the index of refractive decrement, relates the focal length to the decrement. From this information combined with the previous relationships, the fact that

$$f \propto \frac{1}{\lambda^2}$$

can be concluded. This means that the focal length is highly dependent on the wavelength of the x rays passing through the lens. Therefore, in order to achieve high resolutions, the beam of incoming x rays must be monochromatic.

      CRLs are specifically designed to overcome the obstacles of high-energy x-ray imaging. They are comprised of many thin lenses, which serves to reduce the focal length of the lens to reasonable distances, as shown in the focal length equation above. The fact that each individual lens is extremely thin in comparison to its focal length allows the use of the thin lens formula

$$\frac{1}{f} = \frac{1}{d_i} + \frac{1}{d_o}$$

where f is the focal length, d_i is the image distance, and d_o is the object distance, to determine proper placement of the lens.

      Bubble CRL lenses are constructed by filling a tiny glass capillary with a low-Z epoxy (for good transmission of x rays) and then blowing bubbles into it. As shown in Figure 2, the concave epoxy walls left between the bubbles form spherical lenses. The concave shape converges x rays as opposed to diverging visible light because the index of refraction of x rays is less than one. By utilizing a large number of lenses, the focal length can be reduced enough to integrate a lens system onto an existing camera mount on the Omega laser.
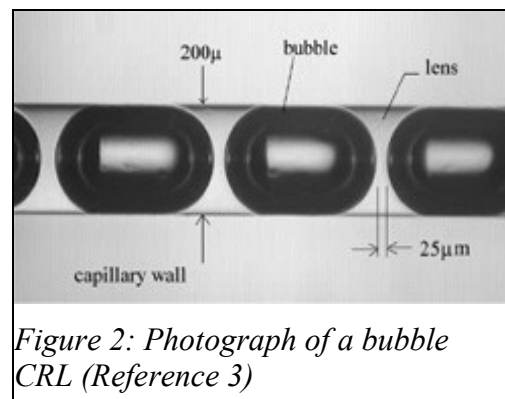

Figure 2: Photograph of a bubble CRL (Reference 3)

The CRL purchased for examination is a 267-lens bubble-style CRL (Figure 3). The diameter of each lens is 200 μm. The total thickness of the combined lenses is 4.47 mm. The exact chemical composition of the epoxy used was not provided by the manufacturer, but considering other epoxies produced by the same manufacturer, the chemical formula was estimated to be $C_{100}H_{200}O_{20}N$. The total lens length is 7.5 cm.
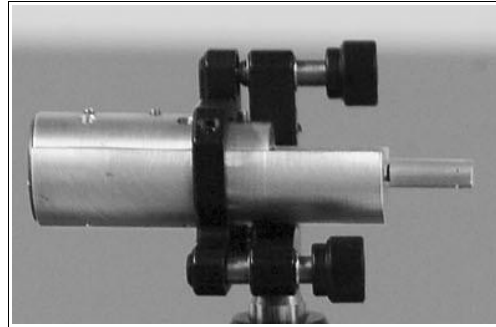

Figure 3: The CRL is held in the aluminum casing protruding from the right side of the V-groove mount

In order to determine the focal length of the lens, calculations were done to compare theoretical lengths versus the data sent from the lens's manufacturer, Adelphi. The values reported by Adelphi were focal lengths of 33 cm at 20.2 keV and 19 cm at 15.4 keV. The focal length was calculated to be 5.26 cm at 8.03 keV. Object and image distances were then

Table 1.	Object and Image Distances Calculated for Different Magnifications at 8.03 keV with a Cu X-ray source
Test Energy (keV)	8.03
Reference Energy (keV)	20.2
Ratio	0.4
Ref Focal Length (cm)	33.3
Test Focal Length (cm)	5.26
Magnification	15
Grid Distance (cm)	5.61
Film Distance (cm)	84.15
Total Distance (cm)	89.76
Magnification	10
Grid Distance (cm)	5.79
Film Distance (cm)	57.85
Total (cm)	63.64
Magnification	5
Grid Distance (cm)	6.31
Film Distance (cm)	31.56
Total (cm)	37.87

calculated for a variety of magnifications as show in Table 1.

At a magnification of 5x, the image needed to be placed 6.31 cm away from the center of the lens. This table was used to determine the placement of the target and the film during test exposures.

When using a bubble CRL, the field of view is very small due to the elongated shape of the lens. Using the formula (Reference 4),

$$D_{abs} = 2\sqrt{R^2 - (\frac{h_{abs} - h}{2})^2}$$

where R is the radius of the opening, *h* is the thickness of the lens, h_{abs} is the total distance between lenses, and D_{abs} is the absorption aperture radius, D_{abs} was determined to be 189.4 µm. Using the field of view formula,

$$\Phi = \frac{2 D_{abs} a}{l}$$

where *a* is the distance from the lens to the object, D_{abs} is the absorption aperture radius, and *l* is the total length of the lens, a field of view of 318 µm at 5x magnification was calculated. This translates to approximately 4.9 milliradians. One consequence of such a small field of view is that the lens system must be placed very carefully in line with its target. This field of view is wide enough to image the fusion core by a large margin. If the claims made by Adelphi Technologies regarding the accuracy of their laser alignment system are correct, the laser sight should put the target within the field of view.

For a preliminary measure of the spatial resolution of the lens, an image taken by Adelphi Technologies with our lens was analyzed (Figure 4). The bright squares correspond to the gaps in the Au grid. The image was taken by a 20.2 keV Rh source. The picture is of a 400 mesh Au grid under 2x magnification. The focal length was reported as 33 cm at that energy. Using an image analysis suite called PV-Wave, the image was rotated, and vertical slices crossing the mesh bars were selected along paths that were relatively clear of artifacts or irregularities. Figure 5 is a plot of one of these slices.
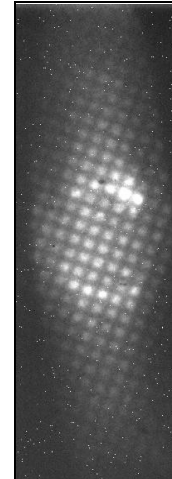

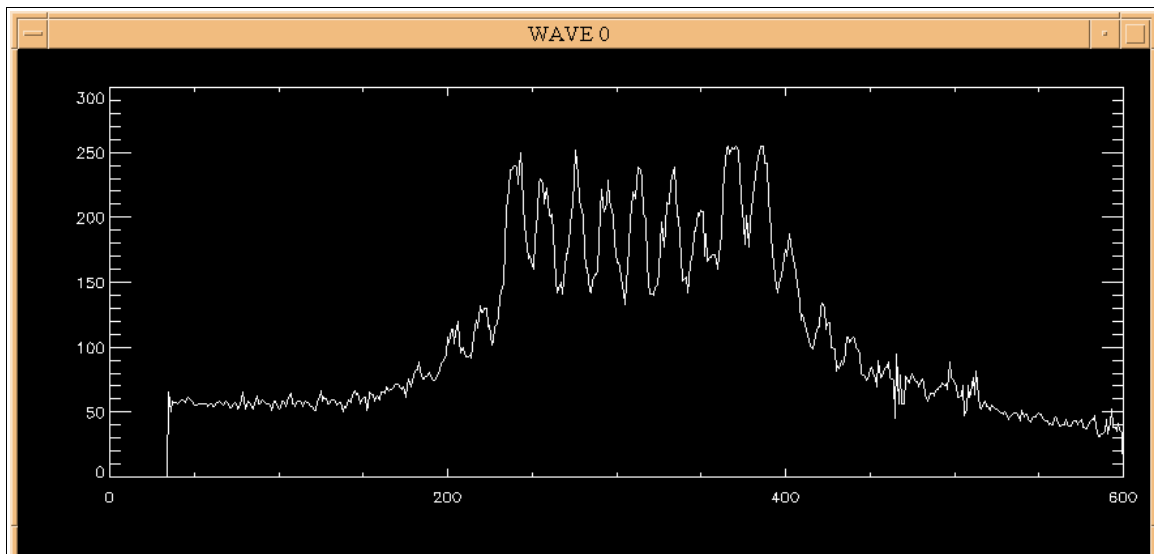*Figure 4: 400 mesh Au Grid, Image by Adelphi Tech.*

Figure 5: Shown is an example plot of pixel brightness on the vertical axis versus position on the horizontal axis. The peaks correspond to the bright patches in Figure 4, and the depressions correspond to the bars of the grid.

The curve was smoothed with a nearest neighbor method for a clearer result, and the derivative of the data was plotted. A perfect resolution would yield an infinite derivative at the boundary of grid bar and back light. To determine how far off infinity this image was, a Gaussian equation was fitted to the boundary areas on the plot and an average was recorded.

The Gaussian equation is

$$G(x) = Ae^{\frac{-1}{2}\left(\frac{x-x_0}{\sigma}\right)^2}$$

where A is the amplitude, x is the position, and σ is a representation of the width, or resolution. The value of σ was converted from pixels to μm and used as a representation of the resolution potential of the lens. Figure 6 shows the absolute value of the derivative graph along with Gaussian curves. By fitting curves to the graph of the derivative it is possible to quantify the width of blur at the edge of each grid bar in the image. Table 2 shows the collective sigma data with an average and standard deviation.
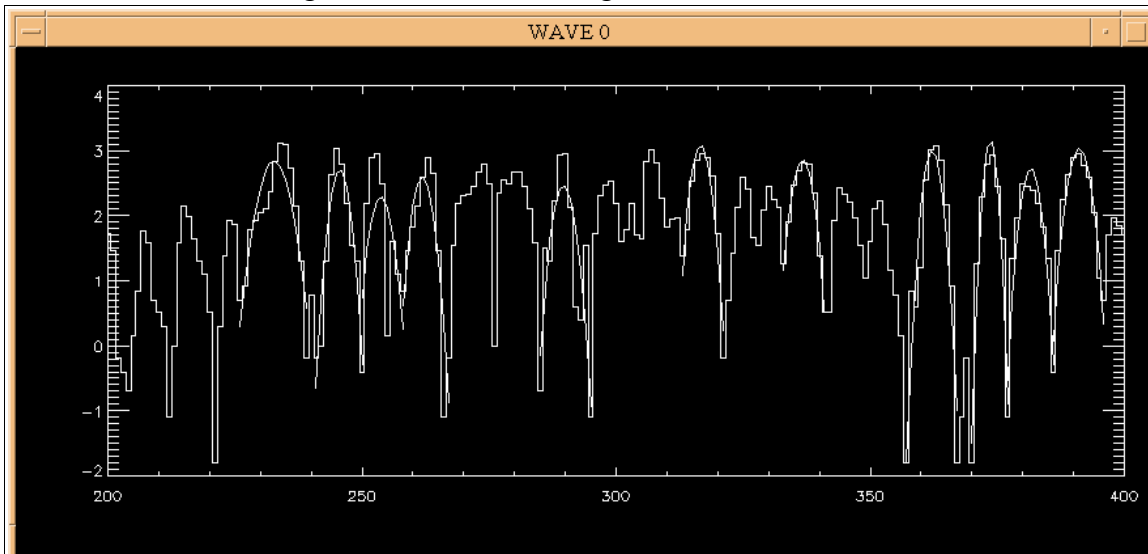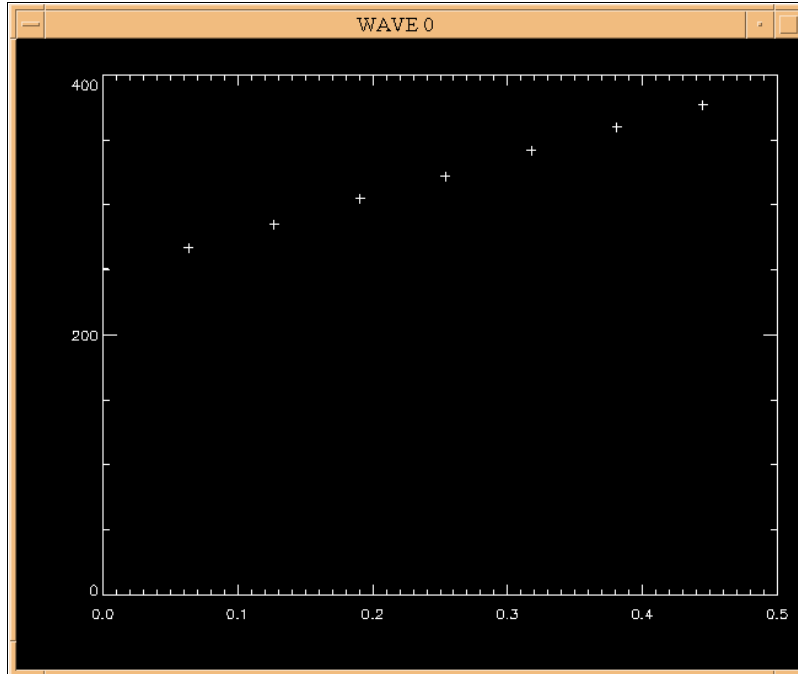

Figure 6: The vertical axis of this graph is the natural log of the brightness. The horizontal axis is pixel position. Gaussian curves are shown over the data.

Table 2   Average Gaussian Curve Fit Variables and Standard Deviations

	σ	X_0	ln A	A
Average:	1.95	312.3	2.8	17.04
STDEV:	0.43	58.31	0.28	4.46

Table 2: This table shows the average Gaussian variables calculated from the PV-Wave output variables along with their standard deviations. These values were used to calculate the spatial resolution and error range.

Because it was a known mesh (400 bars per inch), it was possible to determine the ratio of μm/pixel. To establish the value, the pixel peak i versus i/400 * 2.54x10^4 was

Figure 7: This graph has pixel peak i on the vertical axis versus i/400*2.54x10⁴. The linear slope of the graph is the ratio of μm/pixel

plotted for several consecutive points and the slope was determined (Figure 7). The ratio was determined to be 3.47 μm/pixel. 1.95 average pixels * 3.47 μm/pixel = 6.8 μm resolution. The following formula was used

$$\frac{\Delta\,\text{res}}{\text{res}} = \sqrt{\left(\frac{\Delta\,\text{pixel}}{\text{pixel}}\right)^2 + \left(\frac{\Delta\,\text{u/pixel}}{\text{u/pixel}}\right)^2}$$

with the values Δpixel = .43 (one standard deviation), pixel = 1.95, Δu/pixel = $6.619x10^{-6}$ (as reported by PV-Wave from the linear curve fit, see Figure 7), and u/pixel = 3.47 to determine the error range. The range was determined to be +/- 1.5 μm.

The high energy x-ray apparatus was used with a Cu source with an energy of 8.03 keV. The beam was relatively monochromatic, which is necessary for the best possible resolution. As a target, there were available rings of copper 400 mesh that needed to be placed in an optical mount. A plastic holder was designed to house the grid. The white lens mount can be seen in the left of Figure 8. The mount consisted of a rectangle capable of fitting on the stand, with two concentric holes drilled (one slightly deeper and of smaller radius) and a through-hole. The grid was placed in the smaller hole and held in by a rubber o-ring.
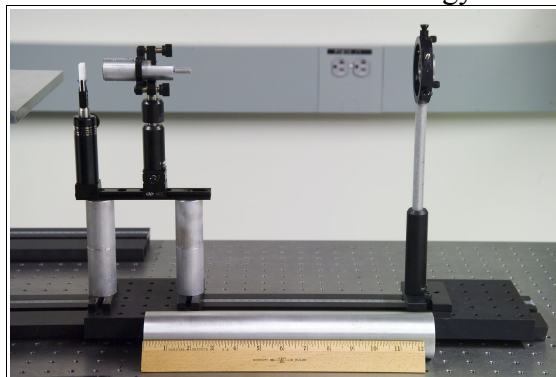
Figure 8: The "telescope" lens system, with (from left to right) grid mount, lens mount, and light-tight film pack containing Biomax x-ray film.

Gaussian Fit on Vertical Data
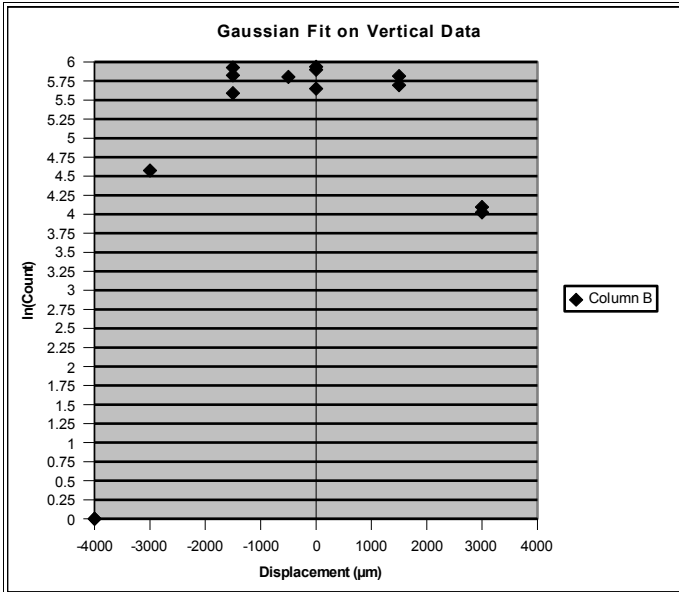
ln(Count)

Displacement (µm)

◆ Column B

Figure 9a: A vertical scan of the beam area showed peak photon counts very close to the initial placement of the diode. The x axis is displacement in µm, and the y axis is the ln of the photons detected in 1 minute

Gaussian Fit on Horizontal Data
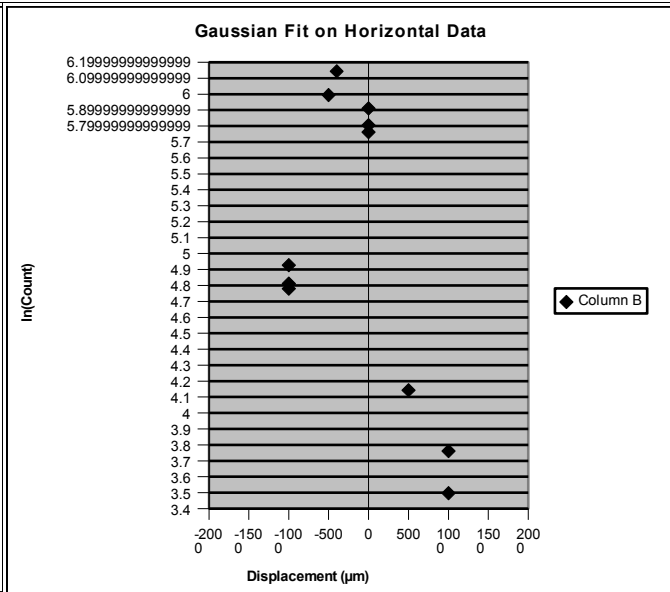
ln(Count)

Displacement (µm)

◆ Column B

Figure 9b: Horizontal scan data. This plot demonstrates the significantly thinner horizontal dimension of the x-ray beam. The peak output is located 500 µm to the left of the initial diode placement.

The lens system was constructed and placed in front of the x-ray beam line. It was necessary to pinpoint the exact beam location since the field of view of the CRL is so small. After using a transit to place the x-ray source in line with the exit slit in the source casing, a pin diode was placed on a set of micron-precision vertical and horizontal motors. The pin diode was used to attempt to locate the beam in both horizontal and vertical dimensions so that proper placement of the lens system would be as simple as possible.

The pin diode was calibrated using the Iron-55 Ka1 and Kb1. A scan across the estimated x-ray beam location was performed, and graphs produced of the photon counts. This allowed for the determination of the peak of the beam intensity, as well as the width of the beam, in order to achieve optimal placement of the lens system (Figure 9). In the vertical dimension, the σ, or graph width, was nearly 1300 µm. In the horizontal dimension, σ was 500 µm. Both were large enough that the beam should encompass the entire view of the lens, with some room for error.

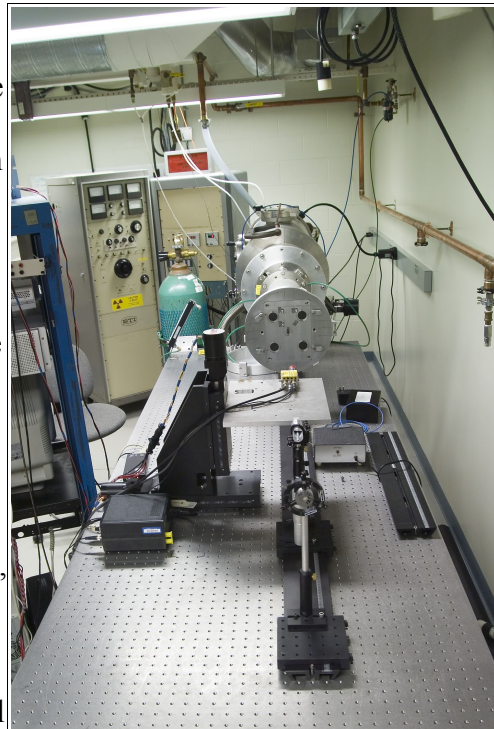After beam determination, the lens system was put into place. The lens and film pack were

Figure 10: The laboratory apparatus, with lens system in the foreground, the pin diode in the middle of the table, and the x-ray source casing.

removed (lens v-groove mount remaining with the tungsten pinhole) and the system was adjusted for maximum transmission. The lens system had been previously aligned by using Adelphi Tech's provided laser alignment system, in which a glass capillary laser of the same diameter as the lens holder was used to aim the lens both at the grid and the film. The laser supposedly has the same field of view as the lens. The laser alignment system was also used to verify alignment with the x-ray source. This method of alignment could potentially cause problems in the future. This alignment procedure relies on the consistency of the placement of the capillary laser and CRL, as well as the stability of the mount. The repeatability of the lens alignment is low, due to the uncertainty of the x-ray beam optical axis itself, as well as the difficulty of placing the lens system's optical axis in line.

Image attempts were mostly unsuccessful. An image was taken through the tungsten pinhole without the lens in place, but even with 3 hour exposure times, no images with the lens in place were achieved. Though potentially a problem of alignment, it was also calculated that with the current x-ray source it was nearly impossible to get an exposure in any reasonable amount of time.

With a field of view of ~300 μm and a magnification of 5x, the total target area on the film is $4.4 \times 10^5 \, \mu m^2$. With the current x-ray source the count rate through the lens was approximately 10 photons per minute. Assuming that an image could be formed from 1 photon per μm^2, it would take 4.4×10^4 minute, or 730 hours. In order to reduce the time to a more reasonable 3 hours, the count rate would need to raise to 44 counts per second or more, a 250x increase.

There are multiple options for improving the count rate. Lowering the magnification to 2x would help, but will still result in unacceptable exposure times. The transmission through the 4470 μm of epoxy at 8.03 keV was determined to be approximately .08 (See Figure 11). A higher energy x-ray source could improve transmission. Improving the intensity of the x-ray source is another possible option. Currently there are no higher energy x-ray sources available at the LLE, and the source had already been optimized for maximum intensity. Very high energy x-rays are available at the medical center of the University of Rochester, but they are not

Figure 11: Transmission vs. photon energy through 4470 μm of epoxy (Reference 5)

monochromatic and therefore would result in a blurry image. A combination of a higher energy source, lower magnification, and time for a very long exposure might be able to generate images for analysis. Another possibility would be collaborating with Cornell University to use their x-ray source facilities, which would be an advantage because higher energies could be achieved. This would also possibly help with the difficult alignment and beam collimation.

The preliminary determination of the resolution to be 6.8 +/- 1.5 microns is good enough to warrant further investigation, whether it be at the LLE, or at Cornell
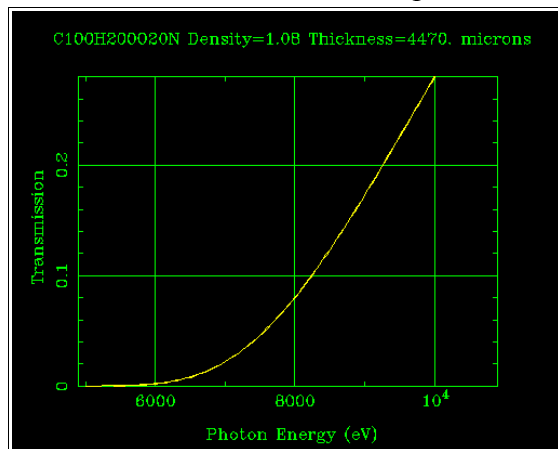
University. The resolution is good enough to image the fusion core with proper alignment. It will be necessary to image a monochromatic x-ray beam. Dopants in the fuel pellets or a monochromator will be necessary to achieve this excellent resolution that has been demonstrated. It was not possible to examine the possibility of distortion such as spherical aberration on an original image. However, there was no sign of distortion in Adelphi's image. For the actual integration on the OMEGA laser system, a single-piece system should be able to be constructed that would fit inside existing camera mounts and be aligned with the implosion location.

References

1. P.A. Bradley, D.C. Wilson, F.J. Swenson, G. L. Morgan, "ICF ignition capsule neutron, gamma ray, and high energy x-ray images," *Review of Scientific Instruments*, Volume 74, Number 3 (2003)

2. Jenkins, F A and White, H E , Fundamentals of Optics, 4E, McGraw-Hill, 1976.

3. Adelphi Technology Inc. http://adelphitech.com/ 8/22/05

4. C.K. Gary, Yu.I. Dudchik, S.A. Pikuzm T.A. Shelkovenko, K.M. Chandler, M.D. Mitchell, D.A. Hammer, "X-ray imaging of an X pinch plasma with a bubble compound refractive lens," *High Temp. Plasma Diagnostics Conf. 2004* – paper E07

5. Eric Gullikson. *X-Ray Interactions With Matter*, http://www-cxro.lbl.gov/optical_constants/filter2.html, 8/21/05

Acknowledgments